

Supporting Information

Using Microemulsions: Formulation Based on Knowledge of their Mesostructure

Michael Gradzielski^{1*}, Magali Duvail², Paula Malo de Molina^{3,4}, Miriam Simon^{1,5},
Yeshayahu Talmon⁵, Thomas Zemb^{1,2}

1: Stranski-Laboratorium für Physikalische und Theoretische Chemie, Institut für Chemie,
Technische Universität Berlin, D-10623 Berlin, Germany

2: ICSM, Université Montpellier, CEA, CNRS, ENSCM, Marcoule, France

3: Centro de Física de Materiales (CFM) (CSIC–UPV/EHU)—Materials Physics Center
(MPC), Paseo Manuel de Lardizabal 5, 20018 San Sebastián, Spain

4: IKERBASQUE - Basque Foundation for Science, María Díaz de Haro 3, 48013 Bilbao,
Spain

5: Dept. of Chemical Engineering and the Russell Berrie Nanotechnology Inst. (RBNI),
Technion-Israel Institute of Technology, Haifa, IL-3200003, Israel

email: michael.gradzielski@tu-berlin.de

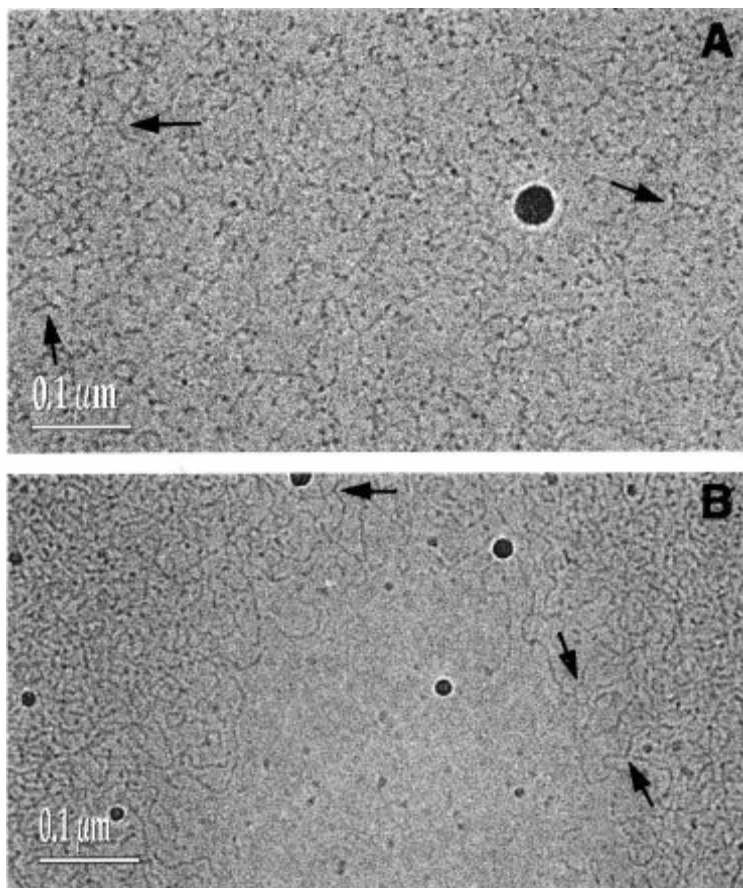


Figure S1. Cryo-TEM images of coexisting microemulsion networks in a sample with $C_{12}E_5$ /water weight ratio of 1.4/98.6 and 0.76 wt% oil at $T = 24.4\text{ }^\circ\text{C}$: (A) dilute (high water content) and (B) concentrated (low water content) phase. In both images one can identify 3-fold junctions (arrows). [156] "Reprinted with permission from [156]. Copyright 1999 American Chemical Society."

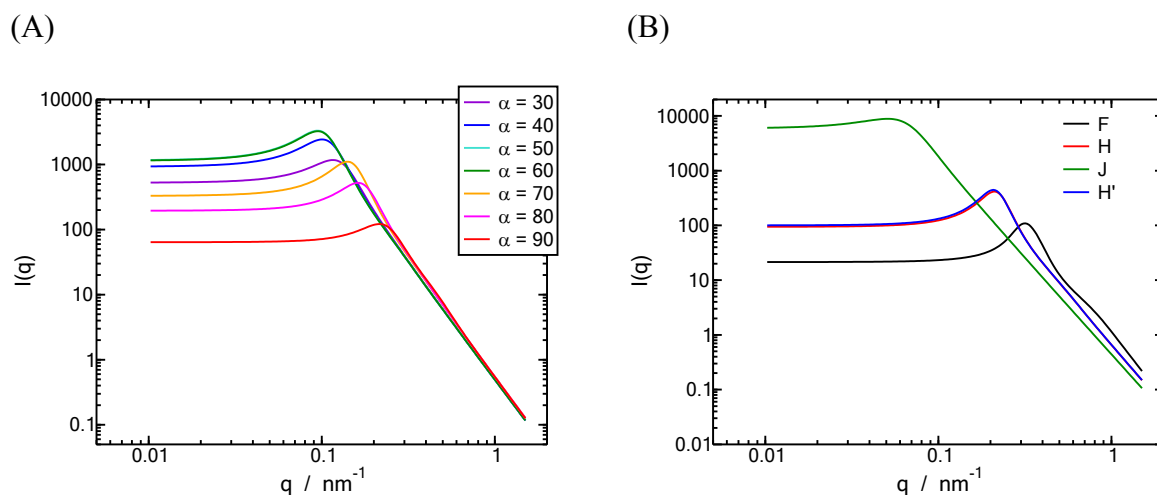


Figure S2. Scattering patterns calculated via the GRF model for the microemulsions shown in (A) Figure 30 as a function of the water-to-oil ratio α , and (B) Figure 31 for different temperatures. Although the oil-to-water ratio has an influence on the microemulsion morphology, it is less marked than the one of temperature. Indeed, changing the temperature clearly change the type of the morphology, as can be seen in (B), since different types of scattering signatures are observed. The scattering curves agree also very well with shape and tendencies seen in the Teubner-Strey²³⁵ and Chen&Choi³³² models described in 3.3.2.

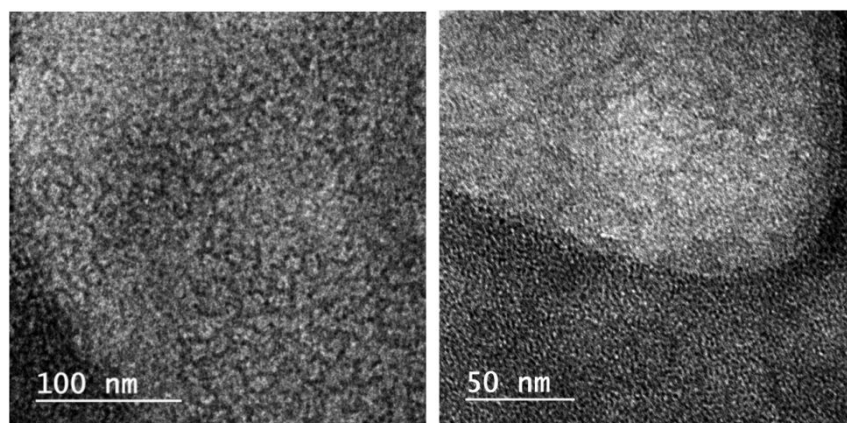


Figure S3. Cryo-TEM images of the microemulsion (middle) phase for the system (water + trihexyltetradecylphosphoniumbis(2,4,4-trimethylpentyl) phosphinate [P6 6 6 14][(iOc)₂PO₂] + n-dodecane) at 298.15 K and atmospheric pressure. (Reprinted from [489], Copyright 2015, with permission from Elsevier.)

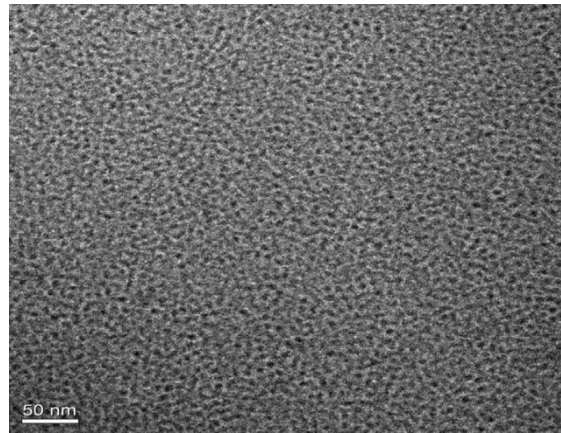


Figure S4. Representative Cryo-TEM micrograph of the O/W microemulsion based on Tween 80 as emulsifier and triacetin as the dispersed oil phase to be used as delivery vehicles of Vemurafenib. (Reprinted from [625, Copyright 2017, with permission from Elsevier.])

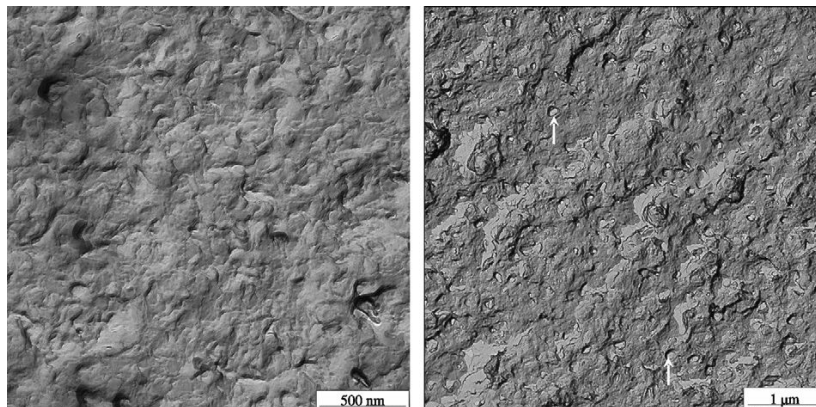


Figure S5. (a) Non-etched freeze fracture EM micrograph of a sample with $\alpha = 0.5$, $\gamma = 0.293$, $\delta = 0.07$. (b) Etched freeze fracture EM micrograph of the same sample. Marked areas indicate holes caused by sublimated ice grains. The observed pattern is typical for a bicontinuous microemulsion structure (Reprinted from [595], Copyright 2008, with permission from Elsevier.)